Nonlinear Dynamics **11:** 107–120, 1996.

Forced Oscillations of a Vertical Continuous Rotor with Geometric Nonlinearity

YUKIO ISHIDA[1], IMAO NAGASAKA[2], TSUYOSHI INOUE[1], and SEONGWOO LEE[1]
[1]*Department of Electronic-Mechanical Engineering, Nagoya University, Furo-cho, Chikusa-ku, Nagoya 464-01, Japan;* [2]*Department of Mechanical Engineering, Chubu University, Matsumoto-cho, Kasugai 487, Japan*

(Received: 20 October 1994; accepted: 17 October 1995)

Abstract. Nonlinear forced oscillations of a vertical continuous rotor with distributed mass are discussed. The restoring force of the rotor has geometric stiffening nonlinearity due to the extension of the rotor center line. The possibility of the occurrence of nonlinear forced oscillations at various subcritical speeds and the shapes of resonance curves at the major critical speeds and at some subcritical speeds are investigated theoretically. Consequently, the following is clarified: (a) the shape of resonance curves at the major critical speed becomes a hard spring type, and (b) among various kinds of nonlinear forced oscillations, only some special kinds of combination resonances have possibility of occurrence.

Key words: Vibration of continuous rotor, nonlinear vibration, subharmonic resonance, combination resonance.

1. Introduction

In the analysis of rotor vibrations, the following two theoretical models are often used. One is a concentrated mass system constituted of a disk and a massless shaft and the other is a distributed mass system constituted of a rotor with a constant diameter. In the theoretical analysis of nonlinear resonances hitherto, the former rotor model has been mainly used. However, the latter model is more suitable for the analyses of, for example, a two-pole generator rotor system which has almost a constant cross section and a shaft which has many similar disks along its axis. In the following, we call the latter model a continuous rotor.

Bolotin analyzed oscillations in an unsymmetrical continuous rotor with directional difference in stiffness, considering nonlinearity due to the geometric stiffening effect [1]. Shaw et al. investigated the stability [2, 3] and chaotic motions [4] of a continuous rotor system with geometric nonlinearity and internal damping. They obtained theoretically the resonance curves of a hard spring type in the neighborhood of a major critical speed. Nonlinear forced oscillations, such as subharmonic resonances and combination resonances, occur when some specific relation holds between the rotating speed and the natural frequencies. As a continuous rotor has an infinite number of natural frequencies, many kinds of such nonlinear subresonance may occur in addition to the resonance at the major critical speeds. In addition, geometric nonlinearity may have its own characteristics different from the clearance type nonlinearity discussed by many researchers.

In this study, we consider a continuous rotor with gyroscopic moment, rotatory inertia and geometric nonlinearity. Transverse shear effects are ignored. We analyze nonlinear forced oscillations [5] which have the possibility of occurrence in a concentrated mass model with quadratic and cubic nonlinearity. Particular attentions are paid to the possibility of occurrence, the shape of resonance curves, and the stability of steady-state oscillations. When the rotor is slender, the natural frequency of the forward whirling mode is almost equal to the absolute

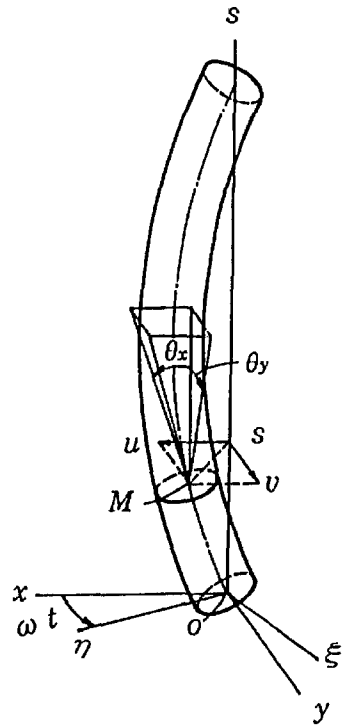

Figure 1. Rotor and coordinates.

value of that of the backward whirling mode and the relation of one-to-one internal resonance holds. However, as we can show that the effect of this internal resonance does not appear in such a system with only symmetrical nonlinearity, we will not consider it here.

These theoretical results are confirmed by experiments.

2. Equations of Motion and Natural Frequencies

2.1. Equations of Motion

Figure 1 shows the theoretical model of an elastic continuous rotor. Both ends of the rotor are supported simply. As the rotor is supported vertically, the gravitational force is not considered in the analysis. The rectangular coordinate system O–xys is fixed in space and O–$\xi\eta s$ rotates at the same angular velocity ω as the rotor. The s-axis coincides with the shaft center line. The rotor has an unbalance $e(e_\xi, e_\eta)$ whose magnitude and angular direction change as a function of s. The rotor is supposed to be slender and shear deformation is neglected. The deflections in Ox- and Oy-directions at time t are denoted by $u(s,t)$ and $v(s,t)$. The equations of motion are given by

$$EI\frac{\partial^4 u}{\partial s^4} + \rho A\frac{\partial^2 u}{\partial t^2} - \frac{\rho A d^2}{16}\left(\frac{\partial^4 u}{\partial s^2 \partial t^2} + 2\omega\frac{\partial^3 v}{\partial s^2 \partial t}\right) + c\frac{\partial u}{\partial t}$$

$$- \frac{EA}{2l}\frac{\partial^2 u}{\partial s^2}\int_0^l \left\{\left(\frac{\partial u}{\partial s}\right)^2 + \left(\frac{\partial v}{\partial s}\right)^2\right\} \mathrm{d}s = \rho A\omega^2(e_\xi \cos\omega t - e_\eta \sin\omega t), \qquad (1)$$

$$EI\frac{\partial^4 v}{\partial s^4} + \rho A\frac{\partial^2 v}{\partial t^2} - \frac{\rho A d^2}{16}\left(\frac{\partial^4 v}{\partial s^2 \partial t^2} - 2\omega\frac{\partial^3 u}{\partial s^2 \partial t}\right) + c\frac{\partial v}{\partial t}$$

$$- \frac{EA}{2l}\frac{\partial^2 v}{\partial s^2}\int_0^l \left\{\left(\frac{\partial u}{\partial s}\right)^2 + \left(\frac{\partial v}{\partial s}\right)^2\right\} \mathrm{d}s = \rho A\omega^2(e_\xi \sin\omega t + e_\eta \cos\omega t), \tag{2}$$

where l is the length of the shaft, d the diameter, A the cross-sectional area, ρ the density, E Young's modulus, I the second moment of area and c the external damping coefficient per unit length. The linear equations of motion corresponding to equations (1) and (2) are given by Eshleman [6] and the nonlinear terms in equations (1) and (2) are in the same form as those obtained by Bolotin [1] and Shaw et al. [2]. By introducing an appropriate unbalance e_0, we adopt the following dimensionless quantities

$$\bar{u} = \frac{u}{e_0}, \quad \bar{v} = \frac{v}{e_0}, \quad \bar{s} = \frac{s}{l}, \quad \bar{e}_\xi = \frac{e_\xi}{e_0}, \quad \bar{e}_\eta = \frac{e_\eta}{e_0},$$

$$\bar{t} = \left(\frac{\pi}{l}\right)^2\left(\frac{EI}{\rho A}\right)^{1/2} \cdot t(=\gamma t), \quad \bar{\omega} = \frac{\omega}{\gamma}, \quad \kappa = \frac{\pi^2 d^2}{16l^2},$$

$$\bar{c} = \frac{cl^4\gamma}{\pi^4 EI}, \quad \alpha = \frac{Ae_0^2}{2I}. \tag{3}$$

In the following, the bars in the dimensionless quantities are omitted for simplicity. Introducing a complex value $z = u + iv$, we get the equation of motion in the dimensionless form

$$\frac{1}{\pi^4}\frac{\partial^4 z}{\partial s^4} + \frac{\partial^2 z}{\partial t^2} - \frac{\kappa}{\pi^2}\left(\frac{\partial^4 z}{\partial s^2 \partial t^2} - 2i\omega\frac{\partial^3 z}{\partial s^2 \partial t}\right) + c\frac{\partial z}{\partial t}$$

$$- \frac{\alpha}{\pi^4}\frac{\partial^2 z}{\partial s^2}\int_0^l \left(\frac{\partial z}{\partial s}\right)\left(\frac{\partial \bar{z}}{\partial s}\right) \mathrm{d}s = \omega^2[e_\xi(s) + ie_\eta(s)]e^{i\omega}, \tag{4}$$

where $\bar{z}$ is a complex conjugate of z.

2.2. Natural Frequencies

Let a natural frequency of the corresponding linear undamped system be p. As the rotor becomes slender, the gyroscopic effect is small ($\kappa \doteqdot 0$). Under this condition the mode shapes can be expressed approximately by

$$\varphi_n(s) = \sin\nu_n \pi s, \tag{5}$$

where $\nu_n = n$ ($n = 1, 2, \ldots$). Therefore, the solution of free oscillation is represented by [7]

$$z(s,t) = Z \sin\nu_n \pi s e^{ipt}. \tag{6}$$

The natural frequencies p are given by the roots of the frequency equations

$$G_n(p) = \nu_n^4 + 2\kappa\nu_n^2\omega p - (1 + \kappa\nu_n^2)p^2 = 0. \tag{7}$$

For each value of ν_n, this equation has two roots p_{fn} and p_{bn}. The positive one p_{fn} is a natural frequency of forward whirling motion and the negative one p_{bn} is that of backward

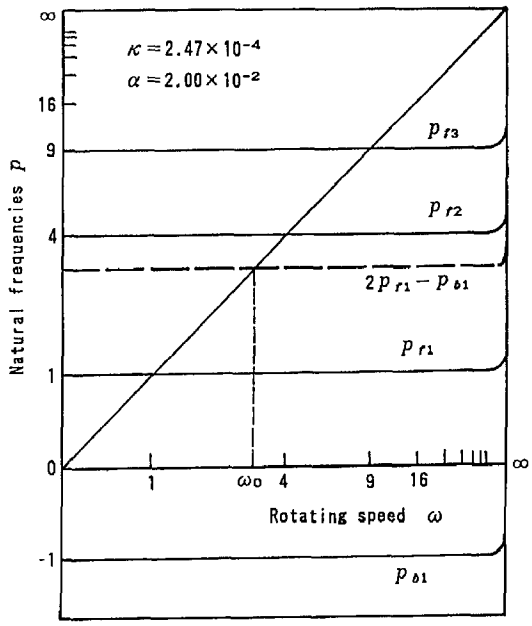

Figure 2. Relation between natural frequencies p_{fn}, p_{bn} and rotating speed ω.

whirling motion. An example of such natural frequencies is shown in Figure 2. In this figure, in order to represent the infinite range $(0, \infty)$ by a finite length a, the scale transformation $\bar{x} = ax/(a + x)$ is adopted, where x is the original scale length and $\bar{x}$ is the length in the figure [8].

2.3. Derivation of Ordinary Differential Equations

It is assumed that the deflections are developed by the eigenfunctions $\varphi_n(s)$ as follows

$$u(s,t) = \sum_{n=1}^{\infty} u_n(t)\varphi_n(s), \qquad v(s,t) = \sum_{n=1}^{\infty} v_n(t)\varphi_n(s). \tag{8}$$

It is also assumed that the unbalances are developed in the same way as follows

$$e_\xi(s) = \sum_{n=1}^{\infty} a_n\varphi_n(s), \qquad e_\eta(s) = \sum_{n=1}^{\infty} b_n\varphi_n(s). \tag{9}$$

Substituting these equations into equation (4) and using the orthogonality of eigenfunctions, we get the following nonlinear ordinary differential equations for modal amplitudes u_n and v_n.

$$\begin{aligned}(1+\kappa\nu_n^2)\ddot{u}_n &+ c\dot{u}_n + 2\kappa\omega\nu_n^2\dot{v}_n + \nu_n^4 u_n + \alpha\nu_n^2 u_n \sum_{j=1}^{\infty}\frac{\nu_j^2}{2}(u_j^2+v_j^2)\\ &= \omega^2(a_n\cos\omega t - b_n\sin\omega t),\end{aligned} \tag{10}$$

$$(1+\kappa\nu_n^2)\ddot{v}_n + c\dot{v}_n - 2\kappa\omega\nu_n^2\dot{u}_n + \nu_n^4 v_n + \alpha\nu_n^2 v_n \sum_{j=1}^{\infty}\frac{\nu_j^2}{2}(u_j^2+v_j^2)$$

$$= \omega^2(a_n \sin\omega t + b_n \cos\omega t) \qquad (n = 1, 2, \ldots). \tag{11}$$

In the following analyses, we will solve these equations by the harmonic balance method.

3. Main Resonances $[p_{fn}]$

In Figure 2, the cross point of the natural frequency curve p_{fn} and the straight line $p = \omega$ gives the major critical speed ω_{fn} for the n-th mode. In the following, we adopt the symbol $[kp_{fm} + lp_{fn} + \cdots]$ $(k, l = \pm 1, \pm 2, \ldots)$ to denote the resonance which occurs at the rotating speed where the relation $\omega = kp_{fm} + lp_{fn} + \cdots$ holds. Let the solutions of the main resonances $[p_{fn}]$ be

$$u_n = P\cos(\omega t + \beta), \qquad v_n = P\sin(\omega t + \beta). \tag{12}$$

Substituting these expressions into equations (10) and (11) under the assumption that P and β change slowly and equating the coefficients of the terms with frequency ω in both sides, we get

$$2\omega P\dot{\beta} = G_n(\omega)P + (1/2)\alpha\nu_n^4 P^3 - \omega^2(a_n \cos\beta + b_n \sin\beta), \tag{13}$$

$$2\omega\dot{P} = -c\omega P - \omega^2(a_n \sin\beta - b_n \cos\beta). \tag{14}$$

By putting $\dot{P} = \dot{\beta} = 0$, we get the steady-state solutions $P = P_0$ and $\beta = \beta_0$. In this paper, the subscript 0 in the variables for amplitudes and phases denotes their steady-state solutions. The stability of these steady-state solutions can be determined by investigating the eigenvalues of the differential equations which are given by considering small variations from these steady-state solutions [9]. Resonance curves are shown in Figure 3. The solid and broken lines represent the stable and unstable solutions, respectively. Resonance curves for three different diameters are drawn. Due to the stiffening effect of geometric nonlinearity, resonance curves become a hard spring type. As the rotor diameter d becomes smaller, the resonance curves incline more strongly. This is because the coefficient α of the nonlinear term in equation (4) is inversely proportional to the double multiplication of d. Here, we must remember that this figure does not reveal the difference of inclination correctly because the rotating speeds are normalized so as to bring the resonance point the value 1 and this scale transformation changes the inclination of these resonance curves. Small circles ○ in Figure 3 are the results of simulation calculated by equations (10) and (11). The approximate solutions agree well with these numerical solutions.

4. The Subharmonic Resonances of Order $1/3[3p_{fn}]$

We assume the solutions of the subharmonic resonance of order 1/3 in the neighborhood of critical speeds $\omega = 3p_{fn}$ as follows

$$u_n = R\cos(\omega_{fn}t + \delta) + P\cos(\omega t + \beta), \tag{15}$$

$$v_n = R\sin(\omega_{fn}t + \delta) + P\sin(\omega t + \beta). \tag{16}$$

Substituting these solutions into equations (10) and (11) and equating the coefficients of the terms with frequency ω_{fn} in the right-hand and left-hand sides, we get the following differential equations for R and δ

$$A_{fn}R\dot{\delta} = R[G_n(\omega_{fn}) + \alpha_{nn}(R^2 + 2P^2)], \tag{17}$$

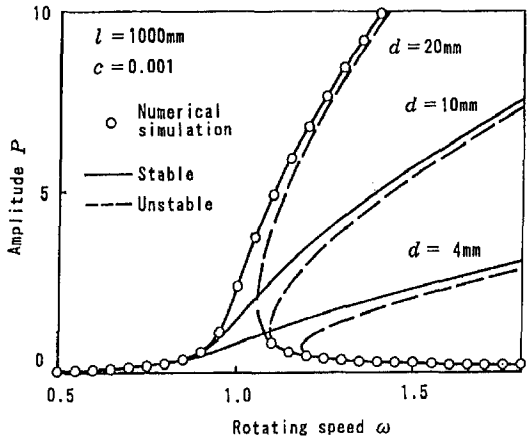

Figure 3. Resonance curves of a main resonance $[p_{f1}]$.

$$A_{fn}\dot{R} = -c\omega_{fn}R, \tag{18}$$

where $\omega_{fn} = (1/3)\omega$, $\alpha_{nn} = (1/2)\alpha\nu_n^4$, $A_{fn} = 2[(1+\kappa\nu_n^2)\omega_{fn} - \kappa\nu_n^2\omega]$. As the steady-state solution P_0 and β_0 of the harmonic component, we adopt the solution of the corresponding undamped linear system. If we put $\dot{R} = \dot{\delta} = 0$ in these equations, algebraic equations for the steady-state solutions are obtained. In this case, only a trivial solution $R_0 = 0$ is obtained and this means that the subharmonic resonance $[3p_{fn}]$ does not occur.

5. Combination Resonances $[2p_{fm} - p_{bn}]$

In the neighborhood of the rotating speed ω_0 where the relationship $\omega = 2p_{fm} - p_{bn}$ (m, n are integers) holds, the vibration components whose frequencies are almost equal to p_{fm} and p_{bn}, respectively, may appear predominantly in addition to the harmonic component with the frequency ω. This oscillation is called a combination resonance or a summed-and-differential harmonic oscillation of the type $[2p_{fm} - p_{bn}]$. The solutions are expressed as follows

$$u_m = R_{fm}\cos\theta_{fm} + P_m\cos(\omega t + \beta_m), \tag{19}$$

$$v_m = R_{fm}\sin\theta_{fm} + P_m\sin(\omega t + \beta_m), \tag{20}$$

$$u_n = R_{bn}\cos\theta_{bn} + P_n\cos(\omega t + \beta_n), \tag{21}$$

$$v_n = R_{bn}\sin\theta_{bn} + P_n\sin(\omega t + \beta_n), \tag{22}$$

where θ_{fm} and θ_{bn} represent the total phase angles corresponding to ω_{fm} and ω_{bn}, respectively. The frequencies of the first terms are given by $\dot{\theta}_{fm}$ or $\dot{\theta}_{bn}$. In the accuracy of the order $O(\varepsilon^0)$, these frequencies are given by

$$\dot{\theta}_{fm} = \omega_{fm} = (p_{fm0}/\omega_0)\omega, \qquad \dot{\theta}_{bn} = \omega_{bn} = (p_{bn0}/\omega_0)\omega, \tag{23}$$

where p_{fm0} and p_{bn0} are the values of p_{fm} and p_{bn} at the rotating speed ω_0. The frequencies given by equations (23) are known.

5.1. CASE OF $m = n$

This is the case that the order of forward whirling mode is the same as that of the backward whirling mode. We assume the solutions in the accuracy of order $O(\varepsilon)$ as follows

$$u_n = R_{fn}\cos(\omega_{fn}t + \delta_{fn}) + R_{bn}\cos(\omega_{bn}t + \delta_{bn}) + P_n\cos(\omega t + \beta_n), \tag{24}$$

$$v_n = R_{fn}\sin(\omega_{fn}t + \delta_{fn}) + R_{bn}\sin(\omega_{bn}t + \delta_{bn}) + P_n\sin(\omega t + \beta_n), \tag{25}$$

where $\theta_{fn} = \omega_{fn}t + \delta_{fn}$ and $\theta_{bn} = \omega_{bn}t + \delta_{bn}$. The following relation holds in the accuracy of order $O(\varepsilon)$,

$$2\dot{\theta}_{fn} - \dot{\theta}_{bn} = 2(\omega_{fn} + \dot{\delta}_{fn}) - (\omega_{bn} + \dot{\delta}_{bn}) = \omega. \tag{26}$$

Substituting equations (24) and (25) into equations (10) and (11) and equating the coefficients of the terms with frequency ω_{fn} or ω_{bn} in the right-hand and left-hand sides, we get

$$\begin{aligned} A_{fn}R_{fn}\dot{\delta}_{fn} &= R_{fn}G_n(\omega_{fn}) + \alpha_{nn}(R_{fn}^2 + 2R_{bn}^2 + 2P_{n0}^2)R_{fn} \\ &\quad + 2\alpha_{nn}R_{fn}R_{bn}P_{n0}\cos(2\delta_{fn} - \delta_{bn} - \beta_{n0}), \end{aligned} \tag{27}$$

$$A_{fn}\dot{R}_{fn} = -c\omega_{fn}R_{fn} + 2\alpha_{nn}R_{fn}R_{bn}P_{n0}\sin(2\delta_{fn} - \delta_{bn} - \beta_{n0}), \tag{28}$$

$$\begin{aligned} A_{bn}R_{bn}\dot{\delta}_{bn} &= R_{bn}G_n(\omega_{bn}) + \alpha_{nn}(2R_{fn}^2 + R_{bn}^2 + 2P_{n0}^2)R_{bn} \\ &\quad + \alpha_{nn}R_{fn}^2P_{n0}\cos(2\delta_{fn} - \delta_{bn} - \beta_{n0}), \end{aligned} \tag{29}$$

$$A_{bn}\dot{R}_{bn} = -c\omega_{bn}R_{bn} - \alpha_{nn}R_{fn}^2P_{n0}\sin(2\delta_{fn} - \delta_{bn} - \beta_{n0}), \tag{30}$$

where $A_{fn} = 2[(1 + \kappa\nu_n^2)\omega_{fn} - \kappa\nu_n^2\omega]$, $A_{bn} = 2[(1 + \kappa\nu_n^2)\omega_{bn} - \kappa\nu_n^2\omega]$, and P_{n0} and β_{n0} are the steady-state solutions in the accuracy of order $O(\varepsilon^0)$ for P_n and β_n, respectively. The equations obtained by putting $\dot{R}_{fn} = \dot{R}_{bn} = \dot{\delta}_{fn} = \dot{\delta}_{bn} = 0$ in equations (27)–(30) give the following two kinds of steady-state solutions R_{fn0} and R_{bn0}.

(i) The case of $R_{fn0} = R_{bn0} = 0$ (trivial solution)

One is a trivial solution $R_{fn0} = R_{bn0} = 0$. The stability of this solution can be investigated if equations (27)–(30) are expressed by the following new variables [9]

$$\begin{aligned} u_{fn} &= R_{fn}\cos\delta_{fn}, \qquad v_{fn} = R_{fn}\sin\delta_{fn}, \\ u_{bn} &= R_{bn}\cos\delta_{bn}, \qquad v_{bn} = R_{bn}\sin\delta_{bn}. \end{aligned} \tag{31}$$

It is proved that this trivial solution is stable at any rotating speed.

(ii) The case of $R_{fn0} \neq 0$ and $R_{bn0} \neq 0$

In this case, steady-state solutions exist even if $\dot{\delta}_{fn}$ and $\dot{\delta}_{bn}$ are not zero. We know from equations (23) and (26) that the condition $2\dot{\delta}_{fn} - \dot{\delta}_{bn} = 0$ is satisfied. Therefore, we introduce a new variable $\psi = 2\delta_{fn} - \delta_{bn}$ and express equations (27)–(30) as follows:

$$\dot{R}_{fn} = [-c\omega_{fn}R_{fn} + 2\alpha_{nn}R_{fn}R_{bn}P_{n0}\sin(\psi - \beta_{n0})]/A_{fn}, \tag{32}$$

$$\dot{R}_{bn} = [-c\omega_{bn}R_{bn} - \alpha_{nn}R_{fn}^2P_{n0}\sin(\psi - \beta_{n0})]/A_{bn}, \tag{33}$$

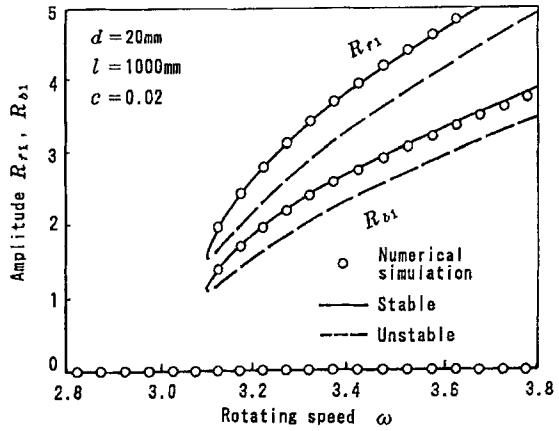

Figure 4. Resonance curves of a combination resonance $[2p_{f1} - p_{b1}]$.

$$\begin{aligned}\dot{\psi} = {} & 2[G_n(\omega_{fn}) + \alpha_{nn}(R_{fn}^2 + 2R_{bn}^2 + 2P_{n0}^2) + 2\alpha_{nn}R_{bn}P_{n0}\cos(\psi - \beta_{n0})]/A_{fn} \\ & - [G_n(\omega_{bn}) + \alpha_{nn}(2R_{fn}^2 + R_{bn}^2 + 2P_{n0}^2) \\ & + \alpha_{nn}(R_{fn}^2/R_{bn})P_{n0}\cos(\psi - \beta_{n0})]/A_{bn}. \end{aligned} \tag{34}$$

The steady-state solutions $R_{fn} = R_{fn0}$, $R_{bn} = R_{bn0}$ and $\psi = \psi_0$ are obtained by putting $\dot{R}_{fn} = \dot{R}_{bn} = \dot{\psi} = 0$ in these equations.

A result is shown in Figure 4. The trivial solution $R_{f10} = R_{b10} = 0$ is stable at any rotating speed. The resonance curves of the nontrivial solutions are a hard spring type and located apart from the trivial solution. It depends on the initial condition which one of these resonance curves appears. As the nonlinear coefficient α becomes large, the resonance curves incline more strongly. As the external damping coefficient c becomes large, the lower end of the resonance curve withdraws upward.

The symbols ○ in Figure 4 represent results of numerical integration of equations (10) and (11), and the theoretical result agrees well with this numerical result. Figure 5 shows time histories obtained by numerical simulations and its spectrum distribution.

5.2. Case of $m \neq n$

In this case, only a trivial solution $R_{fm0} = R_{bn0} = 0$ is obtained. This means that the combination resonance $[2p_{fm} - p_{bn}]$ whose forward and backward mode orders are different does not occur.

6. Combination Resonances $[p_{fl} + p_{fm} - p_{bn}]$

In the neighborhood of the rotating speed $\omega = P_{fl} + P_{fm} - P_{bn}$, the combination resonance $[p_{fl} + p_{fm} - p_{bn}]$ may occur. In this case, the frequencies of vibration components are almost equal to p_{fl}, p_{fm} and p_{bn}, respectively. Similar to equations (23) in the previous section, we represent these frequencies by ω_{fl}, ω_{fm} and ω_{bn}, in the accuracy of $O(\varepsilon^0)$. In these combination resonances, there exist the following two cases.

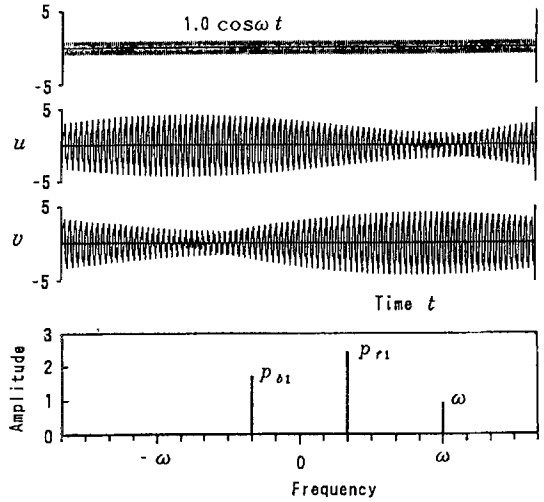

Figure 5. Time histories of a combination resonance $[2p_{f1} - p_{b1}]$.

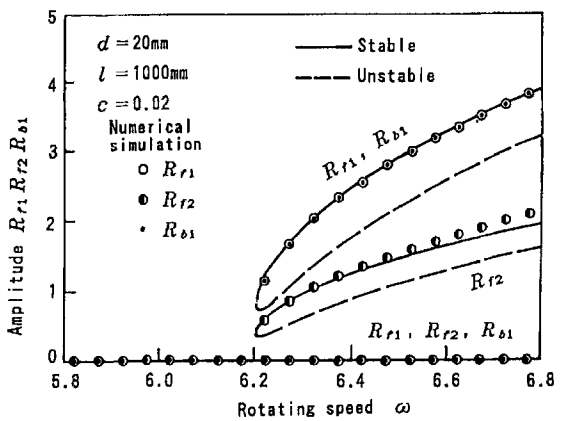

Figure 6. Resonance curves of a combination resonance $[p_{f2} + p_{f1} - p_{b1}]$.

6.1. CASE OF $l = n$ OR $m = n$

Here, we suppose that the relation $l = n$ holds. The solutions in the accuracy of $O(\varepsilon)$ are written as follows

$$u_m = R_{fm}\cos(\omega_{fm}t + \delta_{fm}) + P_m\cos(\omega t + \beta_m), \tag{35}$$

$$v_m = R_{fm}\sin(\omega_{fm}t + \delta_{fm}) + P_m\sin(\omega t + \beta_m), \tag{36}$$

$$u_n = R_{fn}\cos(\omega_{fn}t + \delta_{fn}) + R_{bn}\cos(\omega_{bn}t + \delta_{bn}) + P_n\cos(\omega t + \beta_n), \tag{37}$$

$$v_n = R_{fn}\sin(\omega_{fn}t + \delta_{fn}) + R_{bn}\sin(\omega_{bn}t + \delta_{bn}) + P_n\sin(\omega t + \beta_n). \tag{38}$$

The resonance curves are obtained in the same way as Section 5.1. In the analysis, the variable $\psi = \delta_{fm} + \delta_{fn} - \delta_{bn}$ is adopted for the phase angle.

By the approximate analysis for the steady-state solutions, a trivial solution $R_{fm0} = R_{fn0} = R_{bn0} = 0$ and nontrivial solutions are obtained. An example of resonance curves is shown in Figure 6.

Table 1. Summary of the theoretical analysis.

	Kinds	Linear	Nonlinear
Main resonance	p_{fn}	Occur	Occur
Subharmonic resonance	$2p_{fn}$		×*
	$-2p_{bn}$		×
	$3p_{fn}$		×
	$-3p_{bn}$		×
Combination resonance	$p_{fm}+p_{fn}$		×
	$p_{fm}-p_{bn}$		×
	$-p_{bm}-p_{bn}$		×
	$2p_{fm}+p_{fn}$		×
	$2p_{fm}-p_{bn}$		Occur**
	$p_{fm}-2p_{bn}$		×
	$-2p_{bm}-p_{bn}$		×
	$p_{fl}+p_{fm}+p_{fn}$		×
	$p_{fl}+p_{fm}-p_{bn}$		Occur***
	$p_{fl}-p_{bm}-p_{bn}$		×
	$-p_{bl}-p_{bm}-p_{bn}$		×

*Symbol × means a case that only the steady-state solution with zero-amplitude exists, in other words, this kind of oscillation does not occur.
**This kind of oscillation occurs when $m = n$.
***This kind of oscillation occurs when $l = n$ or $m = n$.

6.2. Case of $l \neq n$ and $m \neq n$

In this case, there exists only a trivial solution $R_{fl0} = R_{fm0} = R_{bn0} = 0$. This means that this kind of combination resonances does not occur.

7. Summary of Theoretical Analysis of Various Kinds of Nonlinear Resonances

We performed the similar analyses of the nonlinear forced oscillations which have possibility to occur in a concentrated mass system with quadratic and cubic nonlinearities [5]. The results are summarized in Table 1. From this table we know the following characteristics:

(a) The main resonances at the major critical speeds appear in both linear and nonlinear systems.
(b) Subharmonic resonances do not occur.
(c) Among various kinds of combination resonances, only two kinds of them occur.

8. Experiments

8.1. Experimental Set-Up

Figure 7 shows the experimental set-up. A uniform elastic rotor with circular cross section is supported vertically. Experiments were performed for two different rotors. They have the same length $l = 800$ mm (this length is the distance between the centers of the upper and the

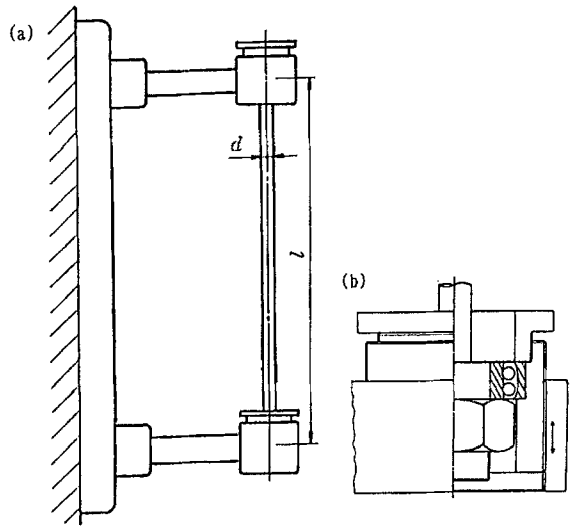

Figure 7. Experimental set-up: (a) rotor system and (b) details of the bearing and the pedestal.

lower bearings) but the different diameters $d = 10$ mm and 4 mm. Both ends of the shaft are supported simply by double row self-aligning ball bearings (#1200). As shown in Figure 7(b), the lower bearing is settled in the bearing box which is movable in the vertical direction in the bearing pedestal. The initial tension in the rotor is adjusted by changing the position of this bearing box. Geometric nonlinearity appeared in the restoring forces of the rotor due to the elongation of the shaft center line.

8.2. Experimental Results

Resonance curves at the major critical speed are shown in Figure 8. Figures 8(a) and (b) are the cases of the rotors whose diameters are $d = 10$ mm and 4 mm, respectively. As the rotor becomes more slender, the inclination of the resonance curve becomes more apparent. We can find clearly a hysteresis phenomenon and jump phenomena in Figure 8(b).

Experimental results on the combination resonance $[2p_{f1} - p_{b1}]$ obtained by the rotor of $d = 4$ mm are shown in Figure 9. Figure 9(a) shows resonance curves for the amplitudes R_{f1} and R_{b1} and Figure 9(b) shows the frequencies $\dot{\theta}_{f1}$ and $\dot{\theta}_{b1}$ and the rotating speed ω. The data $\dot{\theta}_{f1}$ and $\dot{\theta}_{b1}$ are almost on the lines passing through the origin and the relationship $2\dot{\theta}_{f1} - \dot{\theta}_{b1} = \omega$ holds.

9. Comparison with the Results of Concentrated Mass Systems

In the previous paper [5], nonlinear resonances in a concentrated mass rotor system where a disc was mounted on a massless elastic shaft were investigated. The system has four degrees of freedom and natural frequencies are denoted by $p_{f1}, p_{f2}, p_{b1}, p_{b2}$ $(p_{f2} > p_{f1} > p_{b1} > p_{b2})$. The following results were obtained [5].

(a) The nonlinear spring characteristics represented by the quadratic and cubic nonlinearities are divided into the isotropic component $N(0)$ and the anisotropic components $N(1)$, $N(2)$, $N(3)$ and $N(4)$. The planar distribution of the potential energy of the component $N(0)$ does not depend on the direction. However, those of the components $N(1)$, $N(2)$, $N(3)$ and

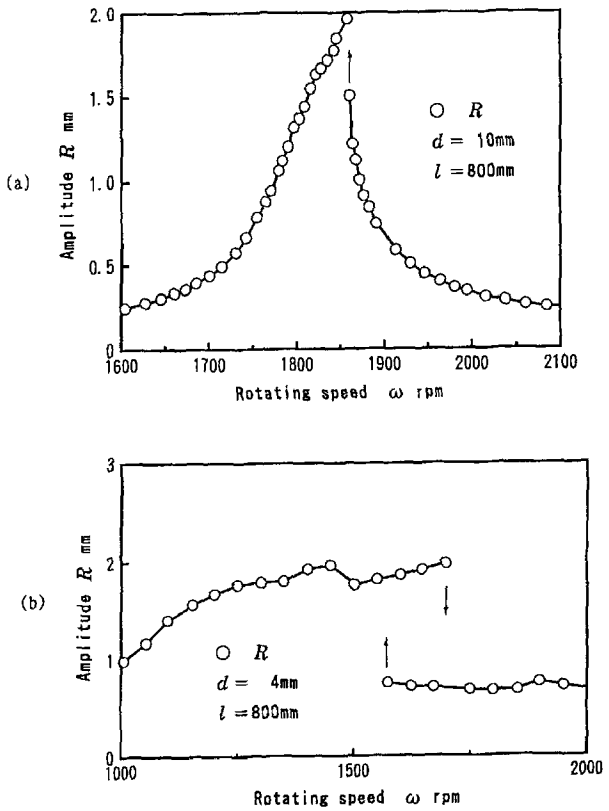

Figure 8. Resonance curves of a main resonance $[p_{f1}]$ (experimental results): (a) case of $d = 10$ mm and (b) case of $d = 4$ mm.

$N(4)$ depend on the direction and its magnitude changes 1, 2, 3 and 4 times periodically, respectively, when the direction changes from 0 to 2π with keeping the magnitude of the deflection and the inclination constant.

(b) The kinds of nonlinear resonance occurring in a rotor system depend on the kinds of these nonlinear components in the system.

(c) If only the isotropic component $N(0)$ exists, the combination resonances $[2p_{fm} - p_{bn}]$ and $[p_{fm} + p_{fn} - p_{bn}]$ $(m, n = 1, 2)$ have a possibility to occur and other kinds of nonlinear resonances do not occur.

The result obtained in this paper is qualitatively the same as that obtained in a concentrated mass system with only the isotropic nonlinear component $N(0)$. Remembering that the geometric nonlinearity treated in this paper is isotropic, this conclusion is understood.

10. Conclusions

Concerning nonlinear resonances of a continuous rotor with geometric nonlinearity, the following results were obtained.

(1) If the movement of the bearings in the direction along the bearing center line is constrained, the geometric nonlinearity appears in the restoring force of the rotor. As the rotor becomes more slender, this geometric nonlinearity becomes apparent and, as a result, the

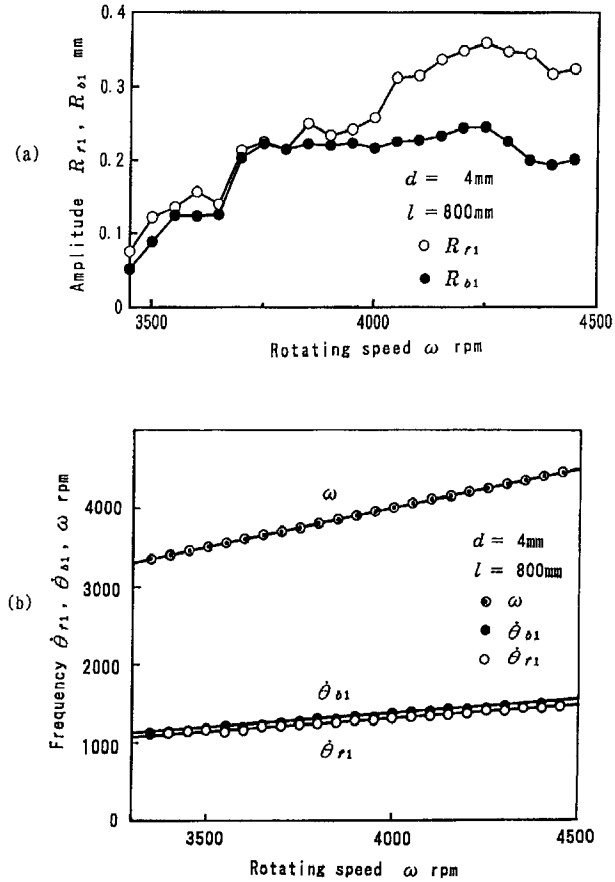

Figure 9. Resonance curves of a combination resonance $[2p_{f1} - p_{b1}]$ (experimental results): (a) amplitudes and (b) frequencies.

resonance curves at the major critical speeds and those of combination resonances are a hard spring type. These characteristics are similar to the case of a nonrotating beam.

(2) Combination resonances $[2p_{fn} - p_{bn}]$ and $[p_{fm} + p_{fn} - p_{bn}]$ occur.

(3) Subharmonic resonances $[2p_{fn}]$, $[-2p_{bn}]$, $[3p_{fn}]$, $[-3p_{bn}]$, and combination resonances $[p_{fm} + p_{fn}]$, $[p_{fm} - p_{bn}]$, $[-p_{bm} - p_{bn}]$ $[2p_{fm} + p_{fn}]$, $[2p_{fm} - p_{bn}(m \neq n)]$, $[p_{fm} - 2p_{bn}]$, $[-2p_{bm} - p_{bn}]$, $[p_{fl} + p_{fm} + p_{fn}]$, $[p_{fl} + p_{fm} - p_{bn}(l \neq n, m \neq n)]$, $[p_{fl} - p_{bm} - p_{bn}]$ and $[-p_{bl} - p_{bm} - p_{bn}]$ do not appear.

(4) In experiments, resonance curves at the major critical speeds were a hard spring type. The inclination of this resonance curve of a rotor with 4 mm diameter was more apparent than that with 10 mm diameter. Among various combination resonances due to symmetrical nonlinearity, only the resonance $[2p_{f1} - p_{b1}]$ was observed.

References

1. Bolotin, V. V., *The Dynamic Stability of Elastic Systems*, Holden-Day, San Francisco, CA, 1964.
2. Shaw, J. and Shaw, S. W., 'Instabilities and bifurcation in a rotating shaft', *Journal of Sound and Vibration* **132**, 1989, 227–244.
3. Shaw, J. and Shaw, S. W., 'Non-linear resonance of an unbalanced rotating shaft with internal damping', *Journal of Sound and Vibration* **147**, 1991, 435–451.

4. Shaw, S. W., 'Chaotic dynamics of a slender beam rotating about its longitudinal axis', *Journal of Sound and Vibration* **124**, 1988, 329–343.
5. Yamamoto, T. and Ishida, Y., 'Theoretical discussion on vibration of a rotating shaft with nonlinear spring characteristics', *Ingenieur Archiv* **46**, 1977, 125–135.
6. Eshleman, R. L. and Eubanks, R. A., 'On the critical speeds of a continuous rotor', *ASME Journal of Engineering for Industry* **91**, 1969, 1180–1188.
7. Dimentberg, F. M., *Flexural Vibrations of Rotating Shafts*, Butterworths, London, 1961.
8. Tondl, A., *Some Problems of Rotor Dynamics*, Publishing House of the Czechoslovak Academy of Sciences, Prague, 1965.
9. Yamamoto, T., Ishida, Y., and Ikeda, T., 'Super-summed-and-differential harmonic oscillation in a symmetrical rotating shaft system', *Bulletin of JSME* **28**, 1985, 679–686.